Competition between second harmonic generation and two-photon-induced luminescence in single, double and multiple ZnO nanorods

Jun Dai,[1] Jian-Hua Zeng,[1] Sheng Lan,[1,*] Xia Wan,[2] and Shao-Long Tie[2]

[1]*Laboratory of Nanophotonic Functional Materials and Devices, School of Information and Optoelectronic Science and Engineering, South China Normal University, Guangzhou 510006, China*
[2]*School of Chemistry and Environment, South China Normal University, Guangzhou 510006, China*
[*]*slan@scnu.edu.cn*

Abstract: The nonlinear optical properties of single, double and multiple ZnO nanorods (NRs) were investigated by using a focused femtosecond (fs) laser beam. The excitation wavelength of the fs laser was intentionally chosen to be 754 nm at which the energy of two photons is slightly larger than that of the exciton ground state but smaller than the bandgap energy of ZnO. Second harmonic generation (SHG) or/and two-photon-induced luminescence (TPL) were observed and their dependences on excitation density were examined. For single ZnO NRs, only SHG was observed even at the highest excitation density we used in the experiments. The situation was changed when the joint point of two ZnO NRs perpendicular to each other was excited. In this case, TPL could be detected at low excitation densities and it increased rapidly with increasing excitation density. At the highest excitation density of ~15 MW/cm^2, the intensity of the TPL became comparable to that of the SHG. For an ensemble of ZnO NRs packed closely, a rapid increase of TPL with a slope of more than 7.0 and a gradual saturation of SHG with a slope of ~0.34 were found at high excitation densities. Consequently, the nonlinear response spectrum was eventually dominated by the TPL at high excitation densities and the SHG appeared to be very weak. We interpret this phenomenon by considering both the difference in electric field distribution and the effect of heat accumulation. It is suggested that the electric field enhancement in double and multiple NRs plays a crucial role in determining the nonlinear response of the NRs. In addition, the reduction in the bandgap energy induced by the heat accumulation effect also leads to the significant change in nonlinear response. This explanation is supported by the calculation of the electric field distribution using the discrete dipole approximation method and the simulation of temperature rise in different ZnO NRs based on the finite element method.

OCIS codes: (190.4180) Multiphoton processes; (190.2620) Harmonic generation and mixing; (160.6000) Semiconductor materials.

References and links

1. R. F. Service, "Will UV lasers beat the blues?" Science **276**(5314), 895 (1997).
2. M. C. Newton, S. J. Leake, R. Harder, and I. K. Robinson, "Three-dimensional imaging of strain in a single ZnO nanorod," Nat. Mater. **9**(2), 120–124 (2010).
3. P. Zu, Z. K. Tang, G. K. L. Wong, M. Kawasaki, A. Ohtomo, H. Koinuma, and Y. Segawa, "Ultraviolet spontaneous and stimulated emissions from ZnO microcrystallite thin films at room temperature," Solid State Commun. **103**(8), 459–463 (1997).

#186348 - $15.00 USD Received 4 Mar 2013; revised 8 Apr 2013; accepted 9 Apr 2013; published 15 Apr 2013

4. O. Mondal and M. Pal, "Strong and unusual violet-blue emission in ring shaped ZnO nanocrystals," J. Mater. Chem. **21**(45), 18354–18358 (2011).
5. D. M. Bagnall, Y. F. Chen, Z. Zhu, T. Yao, S. Koyama, M. Y. Shen, and T. Goto, "Optically pumped lasing of ZnO at room temperature," Appl. Phys. Lett. **70**(17), 2230–2232 (1997).
6. D. C. Look, J. W. Hemsky, and J. R. Sizelove, "Residual native shallow donor in ZnO," Phys. Rev. Lett. **82**(12), 2552–2555 (1999).
7. B. S. Zou, V. V. Volkov, and Z. L. Wang, "Optical properties of amorphous ZnO, CdO, and PbO nanoclusters in solution," Chem. Mater. **11**(11), 3037–3043 (1999).
8. J. Shi, J. Chen, Z. Feng, T. Chen, X. Wang, P. Ying, and C. Li, "Time-resolved photoluminescence characteristics of subnanometer ZnO clusters confined in the micropores of zeolites," J. Phys. Chem. B **110**(51), 25612–25618 (2006).
9. S. Wu, N. Yuan, H. Xu, X. Wang, and Z. A. Schelly, "Synthesis and bandgap oscillation of uncapped, ZnO clusters by electroporation of vesicles," Nanotechnology **17**(18), 4713–4718 (2006).
10. D. Tainoff, B. Masenelli, O. Boisron, G. Guiraud, and P. Mélinon, "Crystallinity, stoichiometry, and luminescence of high quality ZnO nanoclusters," J. Phys. Chem. C **112**(33), 12623–12627 (2008).
11. B. Jin and D. Wang, "Strong violet emission from zinc oxide dumbbell-like microrods and nanowires," J. Lumin. **132**(8), 1879–1884 (2012).
12. Y. Yang, W. Guo, X. Wang, Z. Wang, J. Qi, and Y. Zhang, "Size dependence of dielectric constant in a single pencil-like ZnO nanowire," Nano Lett. **12**(4), 1919–1922 (2012).
13. G. Jacopin, L. Rigutti, A. L. Bugallo, F. H. Julien, C. Baratto, E. Comini, M. Ferroni, and M. Tchernycheva, "High degree of polarization of the near-band-edge photoluminescence in ZnO nanowires," Nanoscale Res. Lett. **6**(1), 501 (2011).
14. J. C. Johnson, H. Yan, R. D. Schaller, P. B. Petersen, P. D. Yang, and R. J. Saykally, "Near-field imaging of nonlinear optical mixing in single zinc oxide nanowires," Nano Lett. **2**(4), 279–283 (2002).
15. J. Zhang, A. Thurber, D. A. Tenne, J. W. Rasmussen, D. Wingett, C. Hanna, and A. Punnoose, "Enhanced dye fluorescence in novel dye–ZnO nanocomposites," Adv. Funct. Mater. **20**(24), 4358–4363 (2010).
16. H. Guo, Z. Lin, Z. Feng, L. Lin, and J. Zhou, "White-light-emitting diode based on ZnO nanotubes," J. Phys. Chem. C **113**(28), 12546–12550 (2009).
17. C. T. Chien, M. C. Wu, C. W. Chen, H. H. Yang, J. J. Wu, W. F. Su, C. S. Lin, and Y. F. Chen, "Polarization-dependent confocal Raman microscopy of an individual ZnO nanorod," Appl. Phys. Lett. **92**(22), 223102 (2008).
18. J. Dai, Z. Fu, S. Lan, X. Wan, S. Tie, V. A. Trofimov, and T. M. Lysak, "Modified threshold of two-photon-pumped random lasing of ZnO nanorods by femtosecond laser ablation," J. Appl. Phys. **112**(6), 063102 (2012).
19. S. Baskoutas and G. Bester, "Transition in the optical emission polarization of ZnO nanorods," J. Phys. Chem. A **115**, 15862–15867 (2011).
20. Z. Wang, X. F. Qian, J. Yin, and Z. K. Zhu, "Large-scale fabrication of tower-like, flower-like, and tube-like ZnO arrays by a simple chemical solution route," Langmuir **20**(8), 3441–3448 (2004).
21. J. W. Zhao, L. R. Qin, Z. D. Xiao, and L. D. Zhang, "Synthesis and characterization of novel flower-shaped ZnO nanostructures," Mater. Chem. Phys. **105**(2-3), 194–198 (2007).
22. X. D. Gao, X. M. Li, and W. D. Yu, "Flowerlike ZnO nanostructures via hexamethylenetetramine-assisted thermolysis of zinc-ethylenediamine complex," J. Phys. Chem. B **109**(3), 1155–1161 (2005).
23. B. E. Urban, P. B. Neogi, S. J. Butler, Y. Fujita, and A. Neogi, "Second harmonic imaging of plants tissues and cell implosion using two-photon process in ZnO nanoparticles," J Biophotonics **5**(3), 283–291 (2012).
24. B. E. Urban, J. Lin, O. Kumar, K. Senthilkumar, Y. Fujita, and A. Neogi, "Optimization of nonlinear optical properties of ZnO micro and nanocrystals for biophotonics," Opt. Mater. Express **1**(4), 658–669 (2011).
25. Y. L. Wu, S. Fu, A. I. Y. Tok, X. T. Zeng, C. S. Lim, L. C. Kwek, and F. C. Y. Boey, "A dual-colored bio-marker made of doped ZnO nanocrystals," Nanotechnology **19**(34), 345605 (2008).
26. S. W. Liu, H. J. Zhou, A. Ricca, R. Tian, and M. Xiao, "Far-field second-harmonic fingerprint of twinning in single ZnO rods," Phys. Rev. B **77**(11), 113311 (2008).
27. M. Chattopadhyay, P. Kumbhakar, C. S. Tiwary, A. K. Mitra, U. Chatterjee, and T. Kobayashi, "Three-photon-induced four-photon absorption and nonlinear refraction in ZnO quantum dots," Opt. Lett. **34**(23), 3644–3646 (2009).
28. J. H. Lin, Y. J. Chen, H. Y. Lin, and W. F. Hsieh, "Two-photon resonance assisted huge nonlinear refraction and absorption in ZnO thin films," J. Appl. Phys. **97**(3), 033526 (2005).
29. D. C. Dai, S. J. Xu, S. L. Shi, M. H. Xie, and C. M. Che, "Efficient multiphoton-absorption-induced luminescence in single-crystalline ZnO at room temperature," Opt. Lett. **30**(24), 3377–3379 (2005).
30. G. P. Zhu, J. Zhu, C. X. Xu, X. Li, J. P. Liu, and Y. P. Cui, "Multi-photon induced ultraviolet emission from hexagram-shaped ZnO nanorods," Appl. Phys., A Mater. Sci. Process. **95**(2), 381–385 (2009).
31. U. Neumann, R. Grunwald, U. Griebner, G. Steinmeyer, and W. Seeber, "Second-harmonic efficiency of ZnO nanolayers," Appl. Phys. Lett. **84**(2), 170–172 (2004).
32. R. W. Boyd, *Nonlinear Optics*, 3rd ed. (Academic Press, 2008).
33. H. D. Deng, G. C. Li, Q. F. Dai, M. Ouyang, S. Lan, V. A. Trofimov, and T. M. Lysak, "Size dependent competition between second harmonic generation and two-photon luminescence observed in gold nanoparticles," Nanotechnology **24**(7), 075201 (2013).

#186348 - $15.00 USD Received 4 Mar 2013; revised 8 Apr 2013; accepted 9 Apr 2013; published 15 Apr 2013

34. R. Xie, D. Li, H. Zhang, D. Yang, M. Jiang, T. Sekiguchi, B. Liu, and Y. Bando, "Low-temperature growth of uniform ZnO particles with controllable ellipsoidal morphologies and characteristic luminescence patterns," J. Phys. Chem. B **110**(39), 19147–19153 (2006).
35. R. Prasanth, L. K. van Vugt, D. A. M. Vanmaekelbergh, and H. C. Gerritsen, "Resonance enhancement of optical second harmonic generation in a ZnO nanowire," Appl. Phys. Lett. **88**(18), 181501 (2006).
36. D. C. Dai, S. J. Xu, S. L. Shi, M. H. Xie, and C. M. Che, "Observation of both second-harmonic and multiphoton-absorption-induced luminescence in ZnO," IEEE Photon. Technol. Lett. **18**(14), 1533–1535 (2006).
37. B. T. Draine and P. J. Flatau, User guide for the discrete dipole approximation code DDSCAT 7.2, arXiv: 1202.3424 (2012).
38. B. Cao, W. Cai, and H. Zeng, "Temperature-dependent shifts of three emission bands for ZnO nanoneedle arrays," Appl. Phys. Lett. **88**(16), 161101 (2006).
39. T. Y. Hou and X. H. Wu, "A multiscale finite element method for elliptic problems in composite materials and porous media," J. Comput. Phys. **134**(1), 169–189 (1997).
40. S. G. S. Beirão, A. P. C. Ribeiro, M. J. V. Lourenço, F. J. V. Santos, and C. A. Nieto de Castro, "Thermal conductivity of humid air," Int. J. Thermophys. **33**(8-9), 1686–1703 (2012).
41. J. Alvarez-Quintana, E. Martínez, E. Pérez-Tijerina, S. A. Pérez-García, and J. Rodríguez-Viejo, "Temperature dependent thermal conductivity of polycrystalline ZnO films," J. Appl. Phys. **107**(6), 063713 (2010).

1. Introduction

As a semiconductor with wide bandgap (E_g ~3.37 eV) and large exciton binding energy (~60 meV), ZnO has attracted great interest in the last two decades due to its potential applications in the fabrication of various functional devices [1–6]. With the rapid development of nanometer science and technology, ZnO nanoobjects in different fashions have been successfully synthesized or fabricated by various chemical or physical methods. These ZnO nanoobjects, including nanoclusters [7–10], nanowires [11–14], nanotubes [15,16], nanorods (NRs) [17–19], and nanoflowers [20–22], have received intensive and extensive studies due to their unique electric, thermotic, cytalytic, mechanical, magnetic and optical properties originating from surface effect or quantum size effect. Among these properties, the optical properties of ZnO nanowires or NRs have been the focus of many studies because this kind of nanoobjects can be easily synthesized and has potential applications in making optoelectronic devices. In recent years, the nonlinear optical properties of ZnO nanoobjects have attracted much attention owing to their possible applications in the field of biophotonics [23–25]. Under the excitation of a femtosecond (fs) laser in the near infrared region, upconverted signals such as second harmonic generation (SHG) [26] and two-photon-induced luminescence (TPL) [27–29] can be generated in ZnO nanoobjects, making them attractive and promising candidates for bioimaging.

In most cases, SHG and TPL are simultaneously present in ZnO nanoobjects excited by fs laser [30, 31]. It implies that some energy of the fs laser is converted to SHG and some is transferred into TPL. Basically, SHG is a second-order nonlinear process and TPL is a third-order one [32]. However, both of them scale quadratically with the intensity of the incident light, making the situation more complicated. Therefore, it is expected that there exists a competition between these two nonlinear optical processes. Very recently, we have investigated the nonlinear optical response of gold (Au) nanoparticles with much different sizes and found a size dependent competition between SHG and TPL [33]. It is revealed that TPL is dominant in small-sized Au nanoparticles in which absorption is much larger than scattering while SHG is dominant in large-sized Au nanoparticles in which scattering is much larger absorption.

Being as a semiconductor, the physical properties of ZnO appear to be much different from those of Au. For example, the wide bandgap plays an important role in determining the electronic transition of carriers and thus the multiphoton-induced absorption in ZnO. In addition, the melting point of ZnO is much higher than that of Au, making it possible to investigate the nonlinear optical properties of ZnO nanoobjects at high excitation densities that may be modified at high temperatures. All these features make the investigation of the nonlinear optical response of ZnO nanoobjects very interesting.

#186348 - $15.00 USD Received 4 Mar 2013; revised 8 Apr 2013; accepted 9 Apr 2013; published 15 Apr 2013

In this article, we will study experimentally the nonlinear optical responses of single, double and multiple ZnO NRs by using a focused fs laser beam. The excitation wavelength of the fs laser was intentionally chosen to be 754 nm at which the energy of two photons is slightly larger than that of the exciton ground state but smaller than the bandgap energy of ZnO. The purpose is to find out the underlying physical mechanism that determines the competition between SHG and TPL. The article is organized as follows. In section 2, we describe the synthesis of ZnO NRs and the experimental setup used to study the nonlinear optical responses of ZnO NRs under the excitation of the fs laser. In section 3, the nonlinear optical properties of single, double and multiple NRs are described in detail. In addition, we compare the electric field distributions in single, double and multiple NRs calculated by using the discrete dipole approximation (DDA) method and discuss their influences on nonlinear optical response. Also, the temperature rise in different ZnO NRs induced by the heat accumulation effect is calculated by using the finite element method and its influence on nonlinear optical response is analyzed. Finally, the main findings of our research work are summarized.

2. Sample preparation and experimental setup

2.1 Synthesis of ZnO NRs

The ZnO NRs used in our study were synthesized by using the method reported previously [34]. The synthesis process for ZnO NRs can be described in three steps. First, 250-mL aqueous solutions of zinc acetate ($ZnAc_2 \cdot 2H_2O$) and triethanolamine (TEC, $N(CH_2CH_2OH)_3$) with molar ratio of 1: 2 were prepared and put inside two dropping funnels. Then, the two solutions were dropped within 2 hours into a three-neck flask filled with water and subjected to a bath at 90°C. Subsequently, the above suspension was continuously stirred for 1 hour. Finally, the suspension containing ZnO seeds was aged for 12 hours at room temperature. After filtration, the residue was washed three times with a lot of acidic and deionized water and dried at 80°C for 24 hours to obtain ZnO NRs. The SEM image of the synthesized ZnO NRs and the TEM image of a single ZnO NR are shown in Figs. 1(a) and 1(b), respectively. The average diameter and length of ZnO NRs were measured to be ~200 nm and ~2 μm.

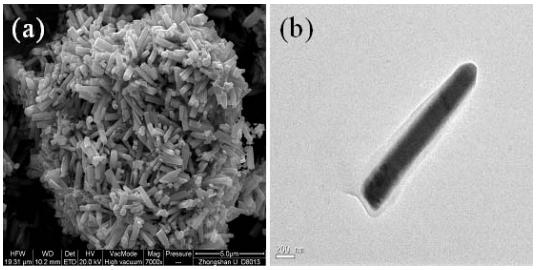

Fig. 1. SEM image of an ensemble of ZnO NRs (a) and TEM image of a single ZnO NR (b).

2.2 Experimental setup

For the characterization of nonlinear optical properties, ZnO NRs were uniformly distributed on a cover glass slide by dropping and dying the aqueous solution of ZnO NRs on the glass slide. The fs laser light from a Ti: sapphire oscillator (Mira 900S, Coherent) with a pulse duration of 130 fs and a repetition rate of 76 MHz was focused on ZnO NRs by using the objective lens (100 × , NA = 1.43) of an inverted microscope (Axio Observer A1, Zeiss). The diameter of the excitation spot was estimated to be ~1 μm. The excitation wavelength of the fs laser was chosen to be 754 nm at which the energy of two photons is slightly larger than that of the exciton ground state but smaller than the bandgap energy of ZnO. All the excitation densities given in the following are the averaged power densities. The peak power

#186348 - $15.00 USD Received 4 Mar 2013; revised 8 Apr 2013; accepted 9 Apr 2013; published 15 Apr 2013

densities can be readily deduced and they are several orders of magnitude larger than the averaged power densities. The emitted nonlinear optical signals (SHG and TPL) were collected by using the same objective lens and directed into a spectrometer (SR-500i-B1, Andor) equipped with a charge-coupled device (CCD) for spectrum analysis. Another CCD connected to the microscope was used to examine the morphology of ZnO NRs and the location of the excitation spot. In all measurements, we have carefully compared the nonlinear optical signals detected at the place with ZnO NRs with those at the place without ZnO NRs (bare glass slide). Under the highest excitation density we used in the experiments, we did not observe any obvious SHG and TPL from the glass slide, indicating that the nonlinear optical response of the glass slide can be neglected. The vertical resolution of the microscope is 200 nm and the maximum nonlinear optical signals were found when the laser light was focused slightly above the glass slide where ZnO NRs were located.

3. Results and discussion

In order to compare the nonlinear optical responses of single, double and multiple ZnO NRs, the as-prepared ZnO NRs were uniformly dispersed in deionized water and dropped on a glass slide. After the evaporation of water, we could easily find single, double and multiple ZnO NRs on the glass slide and a typical example is shown in Fig. 2. The morphologies of the single, double and multiple NRs, whose nonlinear optical properties are presented in the following, are very similar to the typical ones shown in Fig. 2.

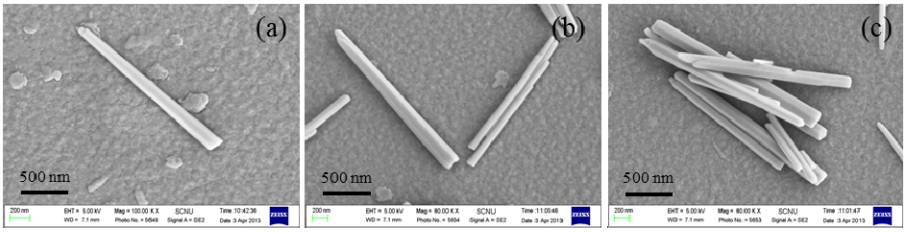

Fig. 2. SEM images of typical single (a), double (b) and multiple (c) ZnO NRs.

3.1 Nonlinear optical response of single ZnO NRs

The CCD image of the single ZnO NR we studied is shown in Fig. 3. The bright spot indicates the position of the excitation spot where the strongest nonlinear optical signal is generated. The nonlinear response spectra of the NR measured at different excitation densities are presented in Fig. 4. In all cases, a narrow peak with a linewidth of ~2.5 nm was observed at 377 nm which was half of the excitation wavelength. The peak wavelength was shifted accordingly when we tuned the excitation wavelength around 754 nm. In addition, the optical signal disappeared completely if we moved the excitation spot out of the NR. Thus, the optical signal at 377 nm was ascribed to the SHG of the NR. This assignment was further confirmed by the excitation density dependent intensity of the optical signal which exhibits a slope of ~1.98, as shown in Fig. 5. Although the energy of two photons at 754 nm is larger than that of the exciton ground state in ZnO, we did not observe any obvious TPL in the nonlinear response spectra even at the highest excitation density of 15 MW/cm^2. Similar results were found at other positions of the NR or in other NRs, indicating that the nonlinear response spectrum of single ZnO NRs is dominated by SHG even in the case when the excitation of TPL is allowed.

#186348 - $15.00 USD Received 4 Mar 2013; revised 8 Apr 2013; accepted 9 Apr 2013; published 15 Apr 2013

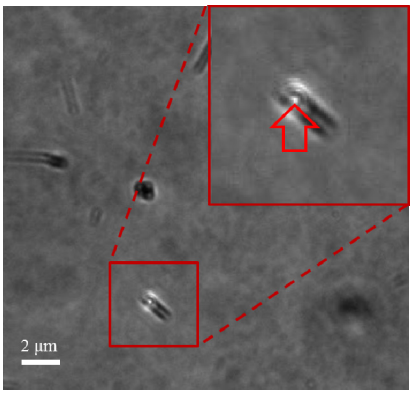

Fig. 3. CCD image of the single ZnO NR we studied. The inset shows the magnified image in which the bright spot (indicated by the arrow) gives the center of the excitation spot where the strongest nonlinear signal was generated.

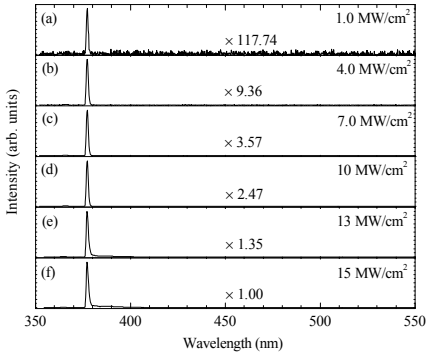

Fig. 4. Evolution of the nonlinear response spectrum of the single ZnO NR with increasing excitation density.

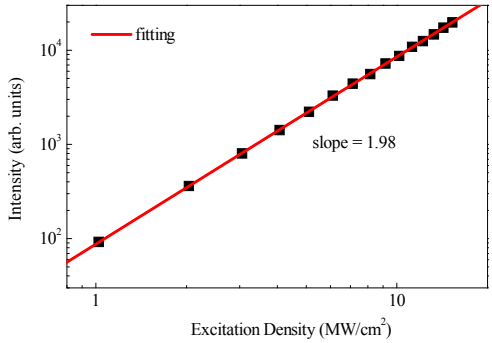

Fig. 5. Excitation density dependent SHG for the single ZnO NR.

3.2 Nonlinear optical response of double ZnO NRs

Now let us examine the nonlinear optical response of two ZnO NRs that are occasionally aligned to be perpendicular to each other, as shown in Fig. 6. The excitation position, which is the bright spot in the image, was chosen at the joint point of the two NRs. The evolution of

#186348 - $15.00 USD Received 4 Mar 2013; revised 8 Apr 2013; accepted 9 Apr 2013; published 15 Apr 2013

the nonlinear response spectrum with increasing excitation density is presented in Fig. 7. In contrast to the narrow SHG peak observed for the single NR, weak TPL was found in the nonlinear response spectrum even at a low excitation density of 1.0 MW/cm^2. Due to the existence of the TPL, the linewidth of the SHG peak located at 377 nm was broadened to be ~6.0 nm. The TPL became obvious at 4.0 MW/cm^2 with a small peak appearing at ~385 nm. At the highest excitation density of 15 MW/cm^2, the intensity of the TPL became comparable to that of the SHG, as can be seen in Fig. 7(f).

In Figs. 7(a)-7(d), one can see a small peak appearing at ~380 nm, as indicated by the arrows. Since the energy of two photons for the pump light was slightly larger than the energy of the exciton ground state, the excitation of excitons into the exciton states was allowed through two-photon absorption (TPA). Most generated excitons first relaxed to the ground state and then to the defect states. Some excitons, however, might recombine radiatively at the ground state. Therefore, TPL is usually composed of the emissions from the exciton ground state and the defect states. In our case, we think that the small peak appearing at ~380 nm was the emission from the exciton ground state. For the single NR, the nonlinear response spectrum was dominated by SHG and the exciton emission was not observed. It is probably due to the resonant energy transfer from exciton emission to SHG proposed in Ref. [35]. For the double NRs, such resonant energy transfer was weakened, leading to the appearance of the exciton emission at low excitation densities.

By fitting the nonlinear response spectra with multiple Gaussian peaks, we were able to extract the integrated intensities of the SHG and TPL at different excitation densities and plot their excitation density dependences, as shown in Fig. 8. Within the excitation density range we used in the experiments, the relationship between the nonlinear optical signals (SHG or TPL) and the excitation density can be classified into three different regimes in which the excitation density dependent nonlinear optical signals exhibit different slopes. In the low excitation density regime (1.0–6.0 MW/cm^2), a slope of ~1.72 was observed for the SHG while a slope close to 2.0 was found for the TPL. In the moderate excitation density regime (6.0–12 W/cm^2), the slope for the SHG was decreased slightly to ~1.53 while that for the TPL was increased rapidly to ~3.23. A gradual saturation of the SHG was observed in the high excitation density regime (12–15 W/cm^2). In sharp contrast, one can see a dramatic increase of the TPL with a slope as large as ~6.30. This phenomenon indicates that the nonlinear optical response of the double NRs is completely different from that of the single NR. In addition, it clearly shows that there exists a competition between SHG and TPL which is dependent strongly on the excitation density although both of them are expected to scale quadratically with the excitation density. The TPL of the double ZnO NRs appearing at ~385 nm is thought to originate from the recombination of electrons with holes in an electron-hole plasma at high excitation densities [3]. It is completely different from the broad emission band centered at ~530 reported previously for other ZnO nanostructures, which is related to the defects levels of oxygen vacancies [35, 36]. It indicates the absence of such defects levels in our ZnO NRs. On the other hand, the energy transfer from SHG to TPL (i.e., the reabsorption of SHG) may occur at high excitation densities.

In Fig. 9, we present the evolution of the ratio of the integrated intensity of the TPL to that of the SHG with increasing excitation density for the double NRs. It can be seen that the ratio begins to increase rapidly at an excitation density of 13 MW/cm^2. At the highest excitation density of 15 MW/cm^2, the integrated intensity of the TPL is nearly one order of magnitude larger than that of the SHG.

#186348 - $15.00 USD Received 4 Mar 2013; revised 8 Apr 2013; accepted 9 Apr 2013; published 15 Apr 2013

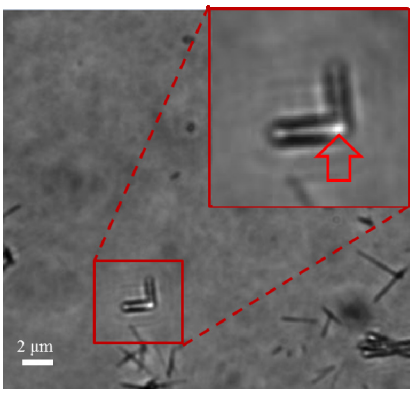

Fig. 6. CCD image of the double ZnO NRs we studied. The inset shows the magnified image in which the bright spot (indicated by the arrow) gives the center of the excitation spot where the strongest nonlinear signal was generated.

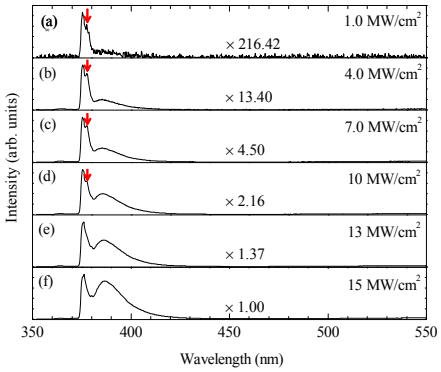

Fig. 7. Evolution of the nonlinear response spectrum of the double ZnO NRs with increasing excitation density.

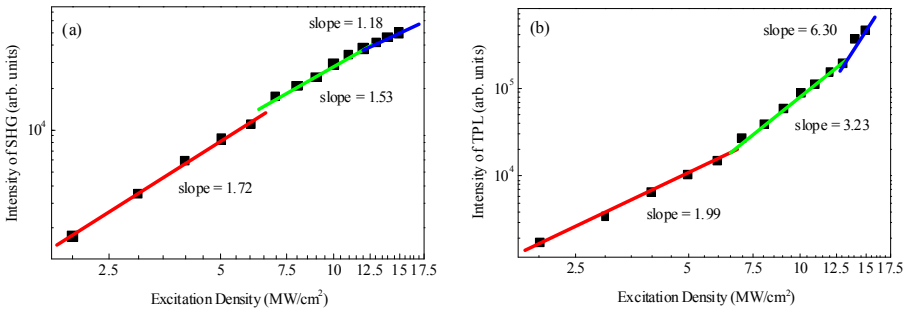

Fig. 8. Excitation density dependent SHG (a) and TPL (b) for the double ZnO NRs.

#186348 - $15.00 USD Received 4 Mar 2013; revised 8 Apr 2013; accepted 9 Apr 2013; published 15 Apr 2013

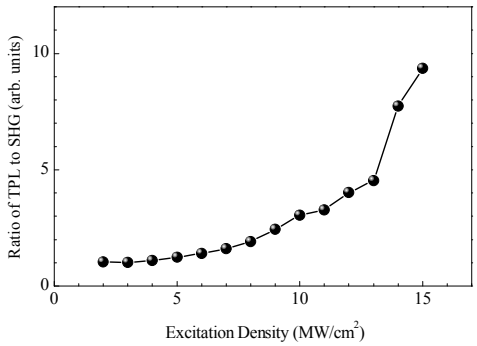

Fig. 9. Evolution of the ratio of the integrated intensity of the TPL to that of the SHG with increasing excitation density for the double ZnO NRs.

3.3 Nonlinear optical response of multiple ZnO NRs

We have seen that the single and double ZnO NRs respond to the excitation of fs laser in completely different ways. The SHG, which is completely dominant in the single NR, is greatly suppressed in the double NRs at high excitation densities. This change in nonlinear optical response makes it interesting to see the nonlinear optical response of multiple NRs. The morphology of the multiple NRs we investigated is shown in Fig. 10. It can be seen that the multiple NRs are composed of several closely packed NRs. Similarly, the bright spot indicates the center of the excitation spot.

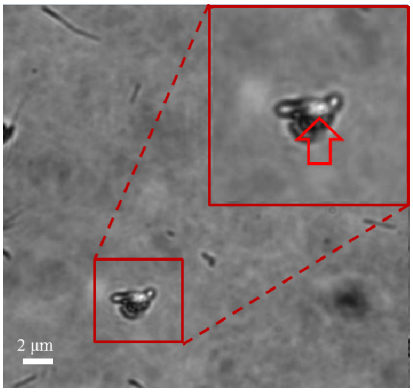

Fig. 10. CCD image of the multiple ZnO NRs we studied. The inset shows the magnified image in which the bright spot (indicated by the arrow) gives the center of the excitation spot where the strongest nonlinear signal was generated.

The evolution of the nonlinear response spectrum of the multiple NRs with increasing excitation density is shown in Fig. 11. At the lowest excitation density of 1.0 MW/cm^2, neither SHG nor TPL was observed. It is thought that the SHG generated in this case is reabsorbed due to the significantly increased absorption cross section in the multiple ZnO NRs. At low excitation densities, the nonlinear response spectra are quite similar to those of the double NRs in which both SHG and TPL are simultaneously present. However, the increase of the TPL with increasing excitation density appeared to be much faster in the multiple NRs than that in the double NRs and the spectrum became dominated by the TPL at an excitation density of 7.0 MW/cm^2. In Fig. 11, it can be seen that the SHG almost disappeared at high excitation densities and the spectrum was governed by the TPL with a broad band. The excitation density dependent SHG and TPL shown in Fig. 12 clearly

#186348 - $15.00 USD Received 4 Mar 2013; revised 8 Apr 2013; accepted 9 Apr 2013; published 15 Apr 2013

indicates the rapid saturation of the SHG and the dramatic increase of the TPL with increasing excitation density. The slope of the SHG is significantly reduced from 1.72 to 0.34 while that of the TPL is increased dramatically from 2.28 to 7.55. If we examine the evolution of the ratio of the integrated intensity of the TPL to that of the SHG with increasing excitation density which is shown in Fig. 13, it is found that the ratio increases from ~5.0 at the lowest excitation density to ~140 at the highest excitation density, implying that the nonlinear response spectrum is completely governed by the TPL.

We think that the weakening of SHG in multiple NRs is not due to the breaking of centrosymmetry because very strong SHG can still be observed in multiple NRs if we choose a longer excitation wavelength at which the excitation of excitons through TPA is not allowed (for example > 770 nm). In this case, the nonlinear response spectrum becomes dominated again by SHG. Therefore, we think that the significant enhancement of local field intensity in multiple ZnO NRs is the main reason responsible for the weakening of SHG, as confirmed by the numerical calculation given in the following.

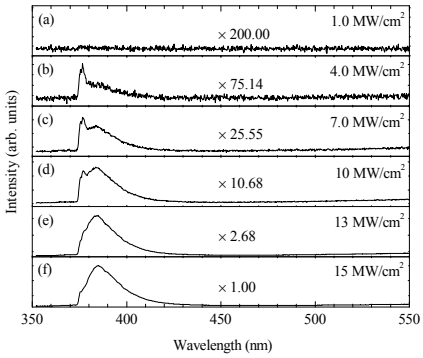

Fig. 11. Evolution of the nonlinear response spectrum of the multiple ZnO NRs with increasing excitation density.

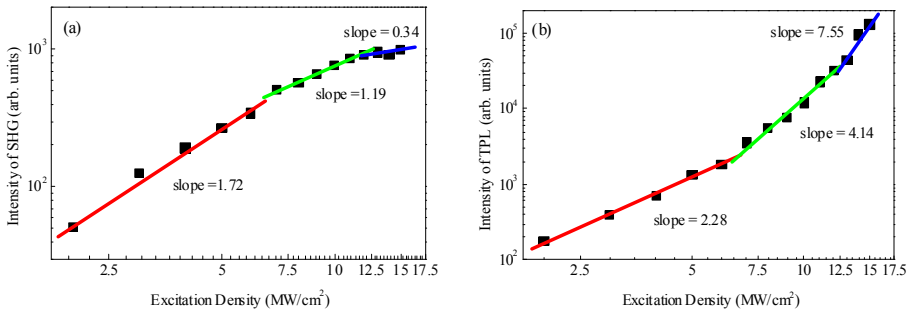

Fig. 12. Excitation density dependent SHG (a) and TPL (b) for the multiple ZnO NRs.

#186348 - $15.00 USD Received 4 Mar 2013; revised 8 Apr 2013; accepted 9 Apr 2013; published 15 Apr 2013

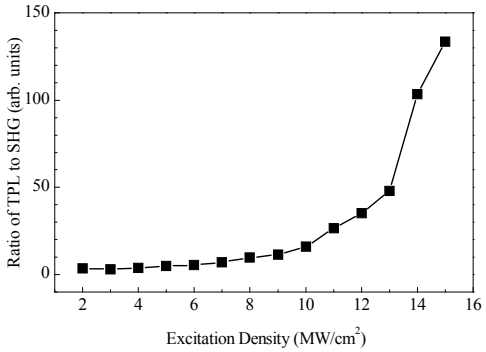

Fig. 13. Evolution of the ratio of the integrated intensity of the TPL to that of the SHG with increasing excitation density for the multiple ZnO NRs.

3.4 Electric field distributions in single, double and multiple ZnO NRs

In order to find out the physical mechanism that is responsible for the change in nonlinear optical response, we have calculated the electric field distributions at the excitation wavelength for single, double, and multiple ZnO NRs by using the discrete dipole approximation (DDA) method [37] and compared them in Fig. 14. For the multiple ZnO NRs, we fixed the number of NRs at 8 and assumed a random distribution of the NRs, as shown in Fig. 14(e).

In the calculation of electric field distribution, the polarization of the incident light was chosen to be along the Y direction, which is the same as that in the experiments. It can be seen that the maximum electric field intensity in the single NR is much weaker as compared to those in the double and multiple NRs. The strongest electric field intensity is achieved in the multiple NRs which is reflected in the large number of "hot spot". Since TPA which leads to TPL is proportional to the fourth power of the local electric field ($\propto E^4$), it is expected that a significant enhancement in TPA and thus in TPL can be achieved in the multiple NRs.

When we compared the local electric field intensities (E^2) for the single and double NRs shown in Fig. 14, an enhancement factor was found to be ~2. Since TPL is quadratically dependent on the intensity of the input light (or the local electric field intensity E^2), the TPL intensity observed at 15 MW/cm^2 for the single NR is expected to be similar to that observed at 4 MW/cm^2 for the double NRs. However, we did not observe such a phenomenon in the experiments. From the competition between SHG and TPL described above, one can see that for double and multiple NRs the saturation of SHG is accompanied by the rapid increase of TPL with a slope much greater than 2.0. For the single NR, the nonlinear optical response is completely dominated by SHG, implying that TPL is greatly suppressed. At the highest excitation density of 15 MW/cm^2, we can see TPL at the long-wavelength side of the SHG although its relative intensity is still much weaker as compared to that of the SHG. In comparison, TPL is enhanced to some extent in the nonlinear optical response of the double NRs. As a result, we began to observe strong TPL even at a low excitation density of 4.0 MW/cm^2.

In the calculated electric field intensities for the single, double and multiple NRs shown in Fig. 14, we can find some hot spots where the large enhancements in electric field intensity are observed. Such hot spots may be resolved by using scanning near field microscope or confocal scanning microscope [14].

#186348 - $15.00 USD Received 4 Mar 2013; revised 8 Apr 2013; accepted 9 Apr 2013; published 15 Apr 2013

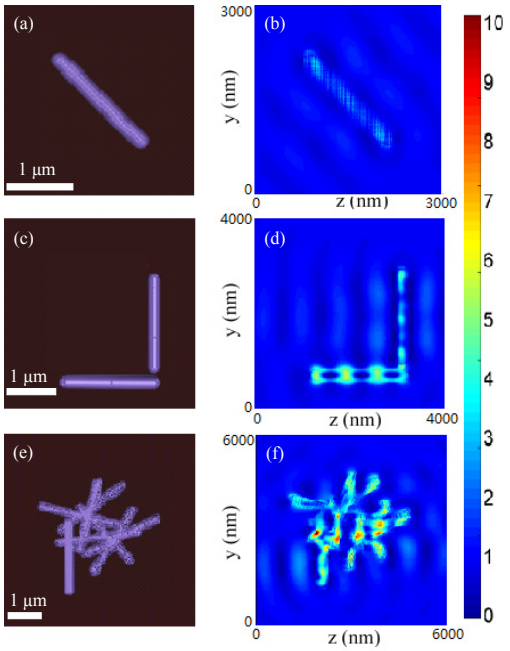

Fig. 14. Calculated electric field intensity distributions in the single, double and multiple ZnO NRs.

3.5 Heat accumulation in single, double and multiple ZnO NRs

Another possible origin that leads to the change in absorption cross section is the temperature rise in the focal volume induced by the heat accumulation effect. The energy carried by the fs laser light is absorbed by ZnO NRs and converted either to photons or to heat through electron-phonon coupling. The heating of ZnO NRs will result in the reduction of bandgap energy and thus the increase in absorption because the excitation of carriers via TPA will occur at high-energy states with large density of states [38]. The increase in absorption will lead to the generation of more heat and the positive feedback results in an avalanche process. In order to evaluate the influence of heat accumulation on the absorption of ZnO NRs, we have calculated the steady temperature distributions on the focal plane at the highest excitation density of 15 MW/cm^2 by using the finite element method [39], as shown in Fig. 15. In the calculation of heat diffusion and temperature distribution, the diameter of the laser spot was assumed to be 1.0 μm and the thermal conductivities of air and ZnO were chosen to be 0.0317 W/m·K and 11 W/m·K [40, 41], respectively. ZnO NRs were assumed to be cylinders with a diameter of 200 nm and a length of 2.0 μm. For the double NRs which are perpendicular to each other, the gap between the two NRs was set to be 100 nm. For the multiple NRs, we chose eight randomly distributed NRs, as shown in Fig. 15(c). Since the thermal conductivity of ZnO is much larger than air, each NR can be considered as a heat source with a constant temperature. The heat released by each NR was determined by the position of the NR and it was proportional to the square of the local laser light intensity. The temperature at the boundary of the calculation region was assumed to be the same as room temperature (300 K). The steady temperature distribution was obtained by numerically solving the heat diffusion equation.

The calculated dependences of temperature rise on excitation density for the single, double and multiple ZnO NRs are presented in Fig. 16. It can be seen that the increase in the number of NRs results in a faster increase in temperature with increasing excitation density

#186348 - $15.00 USD Received 4 Mar 2013; revised 8 Apr 2013; accepted 9 Apr 2013; published 15 Apr 2013

due to the heat accumulation effect. It implies that much higher temperature can be achieved in the multiple NRs as compared to the double or single NRs. As a result, the reduction in bandgap energy is larger for the multiple NRs than that in the double or single NRs. This large decrease in bandgap energy will lead to a significant increase in absorption and thus the strong TPL observed in the experiments. On the other hand, more SHG will be reabsorbed through single photon absorption with the decrease of bandgap energy and converted to luminescence.

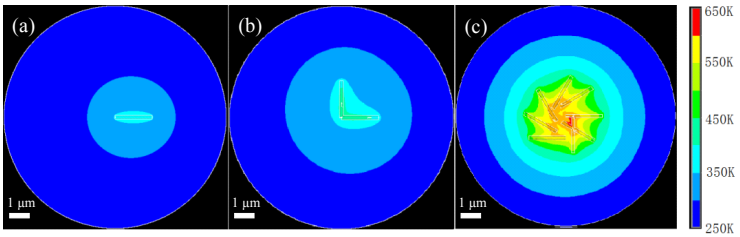

Fig. 15. Heat diffusion and temperature distribution calculated for the single (a), double (b) and multiple (c) ZnO NRs at an excitation density of 15 MW/cm^2.

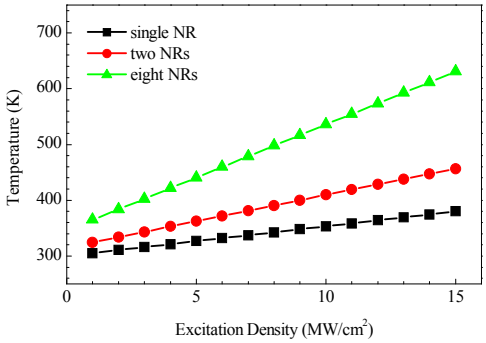

Fig. 16. Excitation density dependent temperature rise induced by the heat accumulation effect for the single, double and multiple ZnO NRs.

4. Summary

We have systematically investigated the nonlinear optical responses of single, double and multiple ZnO NRs under the excitation of fs laser. It was found that for single ZnO NRs only SHG was observed even at the highest excitation density we used. In sharp contrast, a rapid increase in TPL was observed in the double and multiple ZnO NRs and their nonlinear response spectra became completely dominated by TPL at high excitation densities. The difference in nonlinear optical response can be explained by considering both the electric field distribution and the heat accumulation effect. The significant enhancement in electric field intensity in the multiple ZnO NRs, which was confirmed by the DDA calculation, was thought to be responsible for the enhancement in TPA and TPL. On the other hand, the increase in absorption due to the reduction in the bandgap energy induced by the heat accumulation effect also contributed to the significant enhancement in TPL observed at high excitation densities. The understanding of the nonlinear optical processes and the competition between them are helpful for controlling and engineering the nonlinear optical properties of ZnO NRs for device application.

#186348 - $15.00 USD Received 4 Mar 2013; revised 8 Apr 2013; accepted 9 Apr 2013; published 15 Apr 2013

Acknowledgments

The authors acknowledge the financial support from the National Natural Science Foundation of China (Grant No. 51171066), the Ministry of Education (Grant No. 20114407110002) and the program for high-level professionals in the universities of Guangdong province.

#186348 - $15.00 USD Received 4 Mar 2013; revised 8 Apr 2013; accepted 9 Apr 2013; published 15 Apr 2013